Highly Polarizable Metallic Complexes for Nonlinear Optics. Cobaltous Complexes of Unsymmetrical Hydrazone Imine Glyoxal Derivatives

Thierry Thami, Pierre Bassoul, Michel A. Petit, Jacques Simon,* Alain Fort, Marguerite Barzoukas, and Albert Villaeys

Contribution from the ESPCI-CNRS, Chimie et Electrochimie des Matériaux Moléculaires, 10 rue Vauquelin, 75231 Paris Cedex 05, France, and IPCMS-CNRS, Groupe d'Optique Nonlinéaire et d'Optoélectronique, 5 rue de l'Université, 67084 Strasbourg Cedex, France.
Received May 8, 1991

Abstract: The synthesis of 1-(*p*-phenylhydrazono)-2-(phenylimino)ethane derivatives, unsymmetrically substituted in the para positions with an electron acceptor ($-NO_2$) and an electron donor (–OMe or $-NMe_2$), is described, and the corresponding cobaltous complexes are prepared. X-ray diffraction on a single crystal of the dimethylamino complex has been performed (space group: $P\bar{1}$), showing that the coordination site around the cobalt ion is nearly tetrahedral. The complex itself is approximately of C_2 symmetry. The inversion center of the space group transforms one optical isomer into the other. The hyperpolarizability coefficients (β) of the ligands in their cis and trans forms, and those of the neutral cobaltous complexes, have been determined in solution by the electric field induced second harmonic (EFISH) technique. The magnitude of the β value obtained for the complex is larger than the value calculated from the tensorial addition of the molecular hyperpolarizability coefficients of the ligands. The importance of the cation on the nonlinear optical properties of metalloorganic complexes is outlined.

Introduction

The use of organic molecules for second harmonic generation (SHG) in nonlinear optics (NLO) is well documented.[1-3] The NLO properties of standard molecular units may be fairly accurately predicted from the donor/acceptor characteristics of the substituents and from the nature of the conjugation path linking these substituents. Only a few studies have been concerned with metallic coordination complexes.[4-12] In most cases, the metallic moiety is used as an electron donor or electron acceptor subunit. The redox properties of the metallic moieties are not expected to lead, in most examples, to exceptional NLO properties as compared to organic electron donors, e.g., phenoxide, dimethylamino, or electron acceptors such as nitro or cyano. However, there are two respects in which metallic coordination complexes may yield original NLO properties. Firstly, coordination complexes have geometries (tetrahedral, octahedral, square planar) which are extremely difficult to attain with purely organic molecules. Secondly, the molecular orbitals of metalloorganic complexes involve d-orbitals whose symmetry properties are different from those of the s- and p-orbitals found in standard organic chemistry. In organic molecules, the charge-transfer band which is the most efficient for SHG is either uniaxial[1-3] or, more rarely, planar.[13] In conventional disubstituted nitroaniline derivatives (symmetry: C_{2v}), only the term β_{zzz} colinear with the dipole moment is not negligible (Figure 1).

As an example, an organometallic complex with C_2 symmetry may be considered (Figure 1). As a comparison, two independent molecular units having individual hyperpolarizability coefficients β_{MS} arranged in a C_2 symmetry may also be studied.

In the C_2 symmetry with two unidimensional polarization axes, the crossed terms $\beta_{YYZ} = \beta_{ZYY}$ appear. The coefficients may be related to the uniaxial molecular subunit hyperpolarizability coefficients (β_{MS}) by the equations[13]

$$\beta_{ZZZ} = 2\beta_{MS}\cos^3 \alpha$$

$$\beta_{YYZ} = \beta_{ZYY} = 2\beta_{MS}\cos \alpha \sin^2 \alpha$$

where 2α is the angle between the charge-transfer axes of the two molecular subunits (Figure 1). In this approach, the two polarizable subunits are considered to be completely independent, and the overall hyperpolarizability coefficients are calculated from the tensorial sum of the individual hyperpolarizability coefficients. In this model, no enhancement is expected as compared to the response of the individual subunits.

In the case where the two molecular subunits are linked by a transition-metal ion with d-orbitals, five other terms are introduced, which are interrelated far from the resonance by the equations

$$\beta_{ZXX} = \beta_{XXZ}$$

$$\beta_{XYZ} = \beta_{YZX} = \beta_{ZXY}$$

The presence of the d-orbitals may influence SHG in several ways. (i) In the C_2 symmetry, the d–d transitions are symmetrically allowed (A → A and B → B, *z* polarization; A → B, *x*, *y* polarization). These electronic transitions may contribute to the hyperpolarizability coefficients. (ii) The complexation of an ion by the two molecular subunits permits interligand and metal-to-ligand charge-transfer transitions. (iii) The complexation may also favor a delocalization between the donor and the acceptor substituents and therefore enhance the intraligand charge transfer. In all cases, the use of metal complexes induces the presence of three-dimensional charge transfers in NLO, which are unusual, if known, in organic chemistry.

The synthesis of metalloorganic complexes also allows the formation of optically active molecular units, in which the chirality

(1) Chemla, D. S.; Zyss, J. *Nonlinear Optical Properties of Organic Molecules & Crystals*; Academic Press: Orlando, 1987.
(2) Williams, D. J. *Angew. Chem., Int. Ed. Engl.* **1984**, *23*, 690.
(3) Simon, J.; Bassoul, P.; Norvez, S. *New. J. Chem.* **1989**, *13*, 13.
(4) Frazier, C. C.; Harvey, M. A.; Cockerham, M. P.; Hand, H. M.; Chauchard, E. A.; Lee Chi, H. *J. Phys. Chem.* **1986**, *90*, 5703.
(5) Calabrese, J. C.; Tam, W. *Chem. Phys. Lett.* **1987**, *133*, 244.
(6) Coe, B. J.; Jones, C. J.; McCleverty, J. A.; Bloor, D.; Kolinsky, P. V.; Jones, R. J. *J. Chem. Soc., Chem. Commun.* **1989**, 1485.
(7) Green, M. L. H.; Marder, S. R.; Thompson, M. E.; Bandy, J. A.; Bloor, D.; Kolinsky, P. V.; Jones, R. J. *Nature* **1987**, *330*, 360.
(8) Ghosal, S.; Samoc, M.; Prasad, P. N.; Tufariello, J. J. *J. Phys. Chem.* **1990**, *94*, 2847.
(9) Anderson, A. G.; Calabrese, J. C.; Tam, W.; Williams, I. D. *Chem. Phys. Lett.* **1987**, *134*, 392.
(10) Zhang, N.; Jiang, M. H.; Yuan, D. R.; Xu, D.; Tao, X. T. *Chinese Phys. Lett.* **1989**, *6*, 280.
(11) Zhang, N.; Jiang, M. H.; Yuan, D. R.; Xu, D.; Shao, Z. S.; Tao, X. T. *Proc. SPIE-Int. Soc. Opt. Eng.* **1990**, *1337*, 390; **1990**, *1337*, 394.
(12) Warren, L. F. Jr. *Eur. Pat. App. EP* 389,879 **1989**; *Chem. Abstr.* 114: 196055m.
(13) Zyss, J.; Oudar, J. L. *Phys. Rev. A* **1982**, *26*, 2028, 2016.

0002-7863/92/1514-915$03.00/0

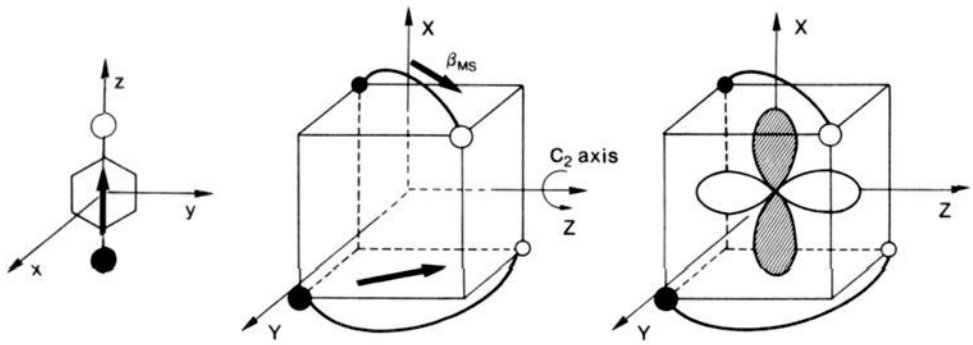

Figure 1. Illustration of one of the geometries found in organometallic chemistry as compared to uniaxial charge-transfer transitions found in organic chemistry.

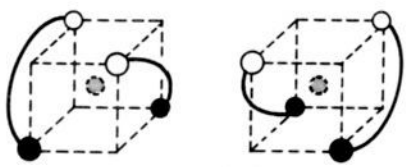

Figure 2. The two optical isomers of C_2 symmetry.

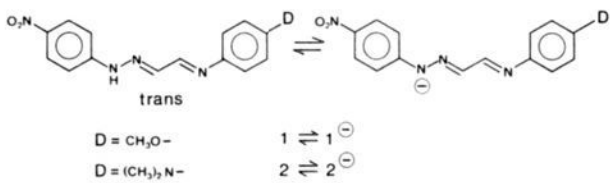

Figure 3. The ligands synthesized and the corresponding anions formed in basic media.

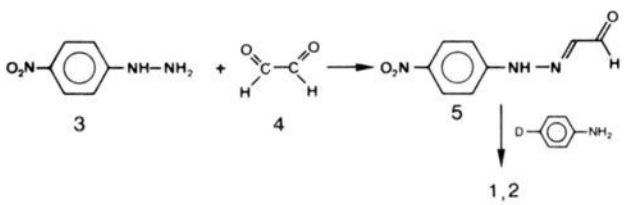

Figure 4. The chemical pathway used to synthesize ligands **1** and **2**.

is strongly associated with electron delocalization (Figure 2).

This paper describes the synthesis of hydrazone imine glyoxal derivatives which are highly polarizable bidentate ligands (Figure 3).

In basic media, the corresponding anions salts are formed. They can be reacted with various metallic salts to give ML_2 complexes (L, ligand; M, first-row divalent metallic ions). The X-ray structure of one of these complexes, $Co^{II}(2^-)_2$, has been determined. The second-order hyperpolarizability coefficients of the various ligands and of the cobaltous complexes have been measured by the electric field induced second harmonic generation (EFISH) method.[14,15]

Synthesis and Characterization of the Ligands. Glyoxal[16] is the key synthon in the chemical pathway leading to ligands **1** and **2** (Figure 4). The synthesis of **1** was previously described,[17] although that of **2** was unknown.

The monosubstituted glyoxal derivative is obtained by reacting *p*-nitrophenylhydrazine with an excess of glyoxal. The yield of the unrecrystallized product is approximately 95%. The reaction of aniline derivatives on glyoxal or glyoxal derivatives is well documented.[18-21] Hydrazine derivatives were chosen instead of aniline derivatives because these latter, substituted with electron acceptor substituents, do not lead to the imino derivative but rather to the corresponding hemiacetals[21] (Figure 5).

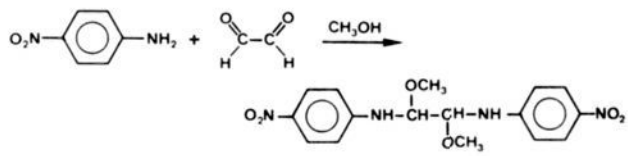

Figure 5. The formation of the hemiacetal derivative.

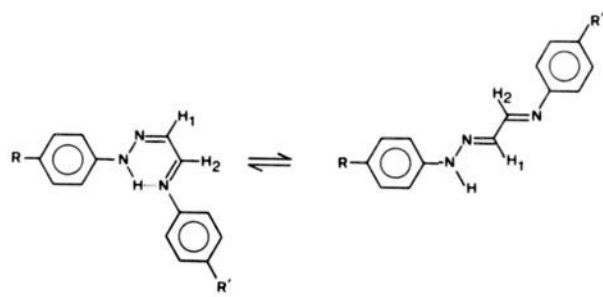

Figure 6. The cis–trans isomerization in ligands **1** and **2**.

Table I. The Cis–Trans Conformation Ratio in Solution for the Ligands **1** and **2** Determined by ^1H NMR[a]

solvent	**1** (D = MeO–)	**2** (D = Me_2N–)
chloroform	70:30	75:25
dioxane	20:80	15:85
DMSO	0:100	0:100

[a] Cis–Trans in %.

The condensation of *p*-dimethylaminoaniline or p-anisidine on the monoadduct **5** leads, in more than a 40% yield, to the final products **1** and **2**.

The optical absorption spectra of ligands closely related to **1** and **2** were already known. Infrared[22] and ultraviolet–visible[17,22,23] absorption spectra showed that such ligands are in a conformational cis–trans equilibrium (Figure 6).

Moreover, tautomeric isomers may be formed by proton transfer; however, such a process is not involved in the case of the nitro derivatives used in the present study.[23]

(14) Levine, B. F.; Bethea, C. G. *J. Chem. Phys.* **1975**, *63*, 2666.
(15) Barzoukas, M.; Josse, D.; Fremaux, P.; Zyss, J.; Nicoud, J. F.; Morley, J. O. *J. Opt. Soc. Amer. B* **1987**, *14*, 977.
(16) Mattioda, G.; Blanc, A. *Ullmann's Encyclopedia of Industrial Chemistry* **1989**, *A12*, 491.
(17) Shandurenko, G. V.; Avramenko, G. V.; Stepanov, B. I. *Zh. Obshch. Khim.* **1980**, *50*, 2559; English translation: *J. Gen. Chem. USSR* **1981**, *50*, 2072. *Zh. Org. Khim.* **1980**, *16*, 751; English translation: *J. Org. Chem. USSR* **1980**, *16*, 659.
(18) Von Pechmann, H.; Schmitz, W. *Ber.* **1898**, *31*, 294.
(19) Beilstein, ed. III, *13*, 1043; ed. III, *13*, 136; ed. II, *13*, 238; ed. I, *13*, 87.
(20) Tom Dieck, H.; Renk, I. W. *Chem. Ber.* **1971**, *104*, 92.
(21) Kliegman, J. M.; Barnes, R. K. *J. Org. Chem.* **1970**, *35*, 3140.
(22) Zaitsev, B. E.; Sheban, G. V.; Shandurenko, G. V.; Avramenko, G. V.; Stepanov, B. I. *Zh. Obshch. Khim.* **1982**, *52*, 49; English translation. *J. Gen. Chem. USSR* **1982**, *52*, 44.
(23) Zaitsev, B. E.; Shandurenko, G. V.; Avramenko, G. V.; Sheban, G. V.; Stepanov, B. I. *Zh. Obshch. Khim.* **1983**, *53*, 2108; English translation: *J. Gen. Chem. USSR* **1984**, *53*, 1902. *Teor. Eksp. Khim.* **1983**, *19*, 584; English translation: *Theor. Exp. Chem.* **1984**, *19*, 539.

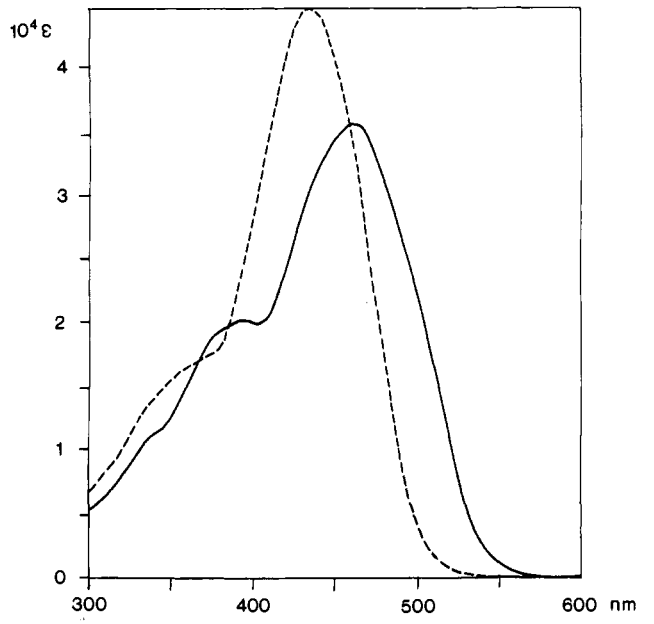

Figure 7. The optical absorption spectra of ligand **2** in $CHCl_3$ (75% cis) (—) and in dioxane (85% trans) (--).

The cis–trans ratio depends on the nature and polarity of the solvent. ^1H NMR studies[24] indicate that the coupling constants between the hydrogen atoms H_1 and H_2 of the glyoxal subunit are 2 and 8 Hz for the cis and trans forms, respectively (Figure 6). The cis form is stabilized by the formation of an internal hydrogen bond, as evidenced by NMR. Similar studies have been carried out on ligands **1** and **2** (Table I).

Furthermore, *E* (Entgegen) and *Z* (Zusammen) isomers are expected, depending on the position of the nitrogen lone pairs of the diimino subunit relative to the hydrogen atoms H_1 and H_2. In Figure 6, the cis-(*Z*–*E*) and trans-(*E*–*E*) isomeric forms, which are probably the most stable, are shown.

The optical absorption spectra of **1** and **2** have been recorded in chloroform, in which the cis form is predominant and in dioxane where the trans form is the major isomer. The results for **2** are shown in Figure 7.

The cis–trans isomerization of **2** leads to a blue shift (25 nm) of the maximum absorption wavelength. At the same time, the extinction coefficients are also slightly altered: $\epsilon_{max}(CHCl_3) = 3.5 \times 10^4$ dm^3·mol^{-1}·cm^{-1} and ϵ_{max}(diox) $= 4.4 \times 10^4$.

In basic media, the ionized products have very different spectra (Figure 8).

In ethanol, the ligands are probably in the trans form. The neutral form of **2** ($\epsilon_{436} = 47\,800$) is blue-shifted compared to 2^- ($\epsilon_{565} = 55\,600$). No absorption peak is observed in the near-IR region (700–2000 nm).

Synthesis and Characterization of the Complexes. The complexation properties of ligands of type **1** and **2** were previously known[25] for the unsubstituted derivatives and for the products substituted with only electron donor groups. No metallic complexes with **1** or **2** were isolated or studied.

The coordination complexes are formed in alcoholic media by first ionizing the ligand with a strong base (potassium ethoxide) and then adding the corresponding metallic salts ($Cu(CF_3SO_3)_2$, $Co(AcO)_2$, $NiBr_2$). The complexes which precipitate from the solution are purified by recrystallization. $M^{II}(\mathbf{1}^-)_2$ ($M^{II} = Cu^{II}$, Ni^{II}, Co^{II}) and $Co^{II}(\mathbf{2}^-)_2$ have all been isolated and characterized (microanalysis, UV–IR spectra).

The optical absorption spectra of $Co^{II}(\mathbf{1}^-)_2$ and $Co^{II}(\mathbf{2}^-)_2$ are shown in Figure 9.

The absorption bands in the range 650–700 nm depend on the nature of the metallic cation: $M(\mathbf{1}^-)_2$, $M = Cu^{II}$ $\epsilon_{679} = 2490$; $M = Ni^{II}$ ϵ_{650} (shoulder); $M = Co^{II}$ $\epsilon_{690} = 2450$. These bands are not present in the ligand spectra; they can therefore be assigned to transitions involving d-metallic orbitals.

The peaks at 1020 nm for $Co^{II}(\mathbf{1}^-)_2$ ($\epsilon = 77$) and $Co^{II}(\mathbf{2}^-)_2$ ($\epsilon = 74$) can be reasonably attributed to d–d transitions.[26] These

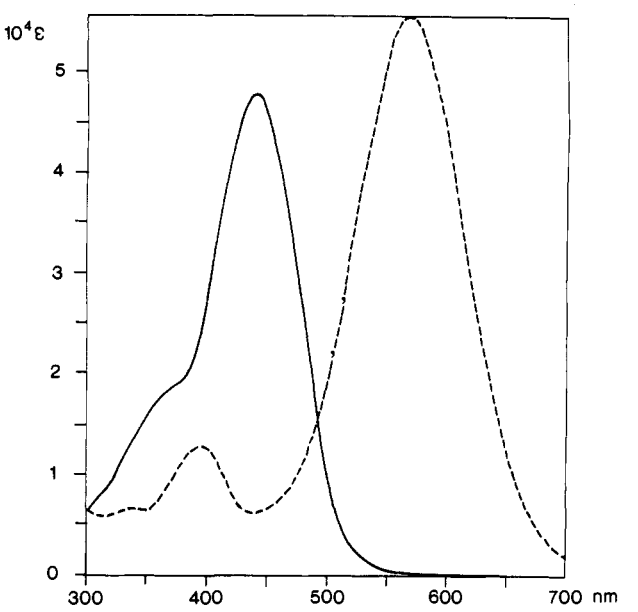

Figure 8. The optical absorption spectra of ligand **2** in the neutral (—) or ionized (--) forms (solvent: ethanol).

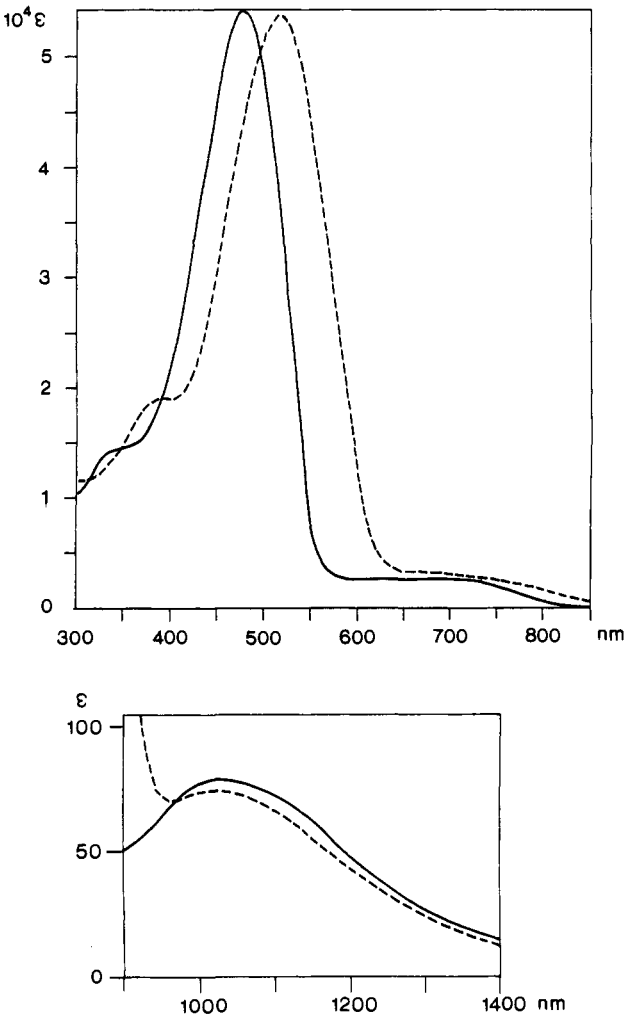

Figure 9. The UV–visible and near infrared absorption spectra of $Co^{II}(\mathbf{1}^-)_2$ (—) and $Co^{II}(\mathbf{2}^-)_2$ (--) in CH_2Cl_2.

(24) McNab, H. *J. Chem. Soc., Perkin Trans. 1* **1980**, *10*, 2200.
(25) Chiswell, B.; O'Reilly, E. J. *Inorg. Chim. Acta* **1979**, *35*, 141.

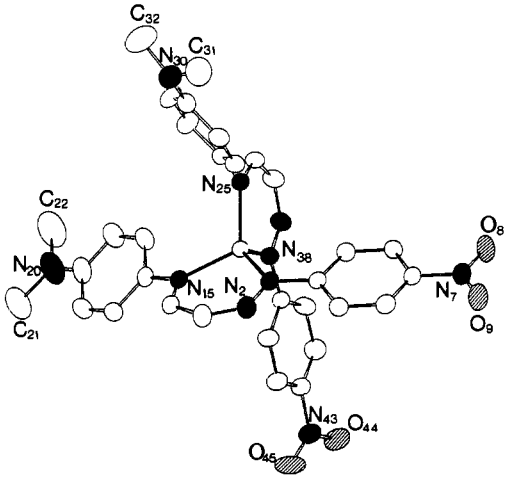

Figure 10. The molecular structure of $Co^{II}(2^-)_2$, obtained by X-ray diffraction.

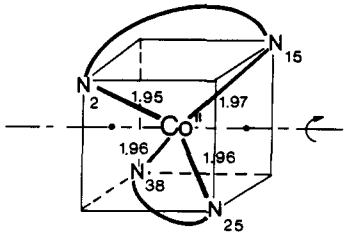

Figure 11. The coordination geometry around the cobaltous ion in the complex $Co^{II}(2^-)_2$. Angles $N_iCo^{II}N_j$: N_2N_{15}, 96.3°; $N_{38}N_{25}$, 95.9°; N_2N_{25}, 118.5°; $N_{38}N_{15}$, 114.5°; $N_{15}N_{25}$, 115.7°; N_2N_{38}, 117.5°.

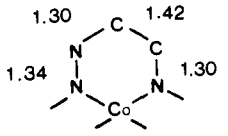

Figure 12. The intraligand bond lengths in $Co^{II}(2^-)_2$. Theoretical values: C—N, 1.47; C=N, 1.29; C—C, 1.54; C=C, 1.33; N—N, 1.40; N=N, 1.26 Å.

bands are, as expected, dependent on the nature of the metal: $Cu^{II}(1^-)_2$, $\epsilon_{1330} = 210$; $Ni^{II}(1^-)_2$, $\epsilon_{1110} = 47$ and ϵ_{1250} (shoulder). No absorption peak is detectable in the region 1400–2000 nm.

The transitions in the region 450–550 nm seem to be present in both the ligands and the complexes; they depend mainly on the nature of the ligand ($Co^{II}(1^-)_2$ $\epsilon_{478} = 54\,200$, $Co^{II}(2^-)_2$ $\epsilon_{518} = 53\,800$) and slightly on the nature of the metal ion ($M(1^-)_2$, M = Cu^{II} $\epsilon_{465} = 39\,700$; M = Ni^{II} $\epsilon_{461} = 46\,300$). (For the aforementioned comparisons, all optical absorption spectra were recorded in CH_2Cl_2.)

Solvatochromic effects ($\Delta\lambda = 15$ nm) have been observed in solvents such as chloroform, dioxane, ether, etc. for the transitions in the regions 450–550 and 650–700 nm. A quantitative treatment of the data[27] was, however, unsuccessful due to the overlap of the various bands.

The structure of $Co^{II}(2^-)_2$ was determined by X-ray diffraction on a single crystal. The space group ($P\bar{1}$) is centrosymmetric, demonstrating the presence of a racemic mixture of the two optical isomers within the crystal. The cobaltous ion is coordinated by four nitrogen atoms in a distorted tetrahedral coordination site (Figure 10).

The Co^{II}–N bond lengths are almost equal (1.96 Å). The intraligand bond angles $NCo^{II}N$ (96°) are smaller than the interligand bond angles (115°–118°). The coordination site of the metal ion is very close to a C_2 symmetry (Figure 11).

The values of the intraligand bond lengths (Figure 12) show a delocalization of the double bonds, as all are found to be intermediate between single and double bond lengths.

The diimino moieties (—N⁻—N=CH—CH=N—) of the ligands are planar. The dihedral angle between the planes formed by the coordinating heteroatoms and the metal ion is approximately 90° (angle between the planes $N_2Co^{II}N_{15}$ and $N_{25}Co^{II}N_{38}$, 89.9°; angle between the two molecular planes, 89.7°).

Table II. The Ground-State Dipole Moments of Ligands **1** and **2** (Solvents $CHCl_3$ (Cis Isomer Predominant) and Dioxane (Trans Isomer Predominant))

	μ (D)	
	μ_c	μ_t
1 (D = MeO–)	8 ± 2	5 ± 1
2 (D = Me_2N–)	10 ± 1	8 ± 1

Table III. Dipole Moments of the Complexes $Co^{II}L_2$ (L = Anion of the Ligands **1** and **2**)

	μ (D)[a]			
	dioxane	chloroform	benzene	μ (D)[b]
$Co^{II}(1^-)_2$ (–OMe)	12.3 ± 0.6	12.0 ± 0.6	11.4 ± 0.6	12 ± 1.5
$Co^{II}(2^-)_2$ (–NMe_2)	14.0 ± 0.7	14.5 ± 0.8		14 ± 1.5

[a] Measured at 10 kHz. [b] Calculated from $\mu = \sqrt{2}\mu_c$.

Determination of the Ground-State Dipole Moments. The determinations of the ground-state dipole moments of the ligands **1** and **2**, and of the corresponding complexes, were performed in chloroform and dioxane (see Experimental Section). The solutions of the ligands contain a mixture of the cis and trans isomers. An additivity law has been used to calculate the respective ground-state dipole moments[28] of the trans and cis isomers, respectively

$$\frac{4\pi}{9kT}\mathcal{N}\,(x_t\mu_t^2 + x_c\mu_c^2) = P_{tc}$$

containing the variables μ_t, μ_c, ground-state dipole moments; x_t, x_c, mole fractions of the corresponding isomers; P_{tc}, molar polarization of the mixture; and $\mathcal{N}$, Avogadro's number.

The cis/trans ratio of the isomers does not vary significantly with the overall concentration. The results are shown in Table II.

The dipole moments of **2** are larger than those of **1**, as expected from the stronger electron donor ability of the dimethylamino group. The trans isomers are, in both cases, less polar than the corresponding cis isomers.

The ground-state dipole moments of the complexes as a function of the solvent are given in Table III.

The dipole moments of the complexes may be determined theoretically by assuming a vectorial contribution of the dipole moments of the two ligands in their cis form. The calculated values are in very good agreement with the experimental determinations, showing that the complexation does not drastically affect the ground-state electronic distribution of the ligands.

The errors on the values of the dipole moments are 10–20% for the ligands and 5% for the complexes.

Nonlinear Optical Properties of the Ligands and of the Complexes. The EFISH method[14,15] has been used to determine the second-order hyperpolarizability coefficients β of the ligands and of the complexes in solution. By this method, the vector part of the hyperpolarizability tensor is measured.[29] If the Kleinman relationships are applied

$$\beta_z = \beta_{zzz} + \beta_{zxx} + \beta_{zyy}$$

where z is the direction of the permanent dipole of the molecule.

The charge transfer in each of the ligands may be considered as uniaxial ($\beta_{zxx} = 0$, $\beta_{zyy} = 0$) or planar ($\beta_{zxx} = 0$, $\beta_{zyy} \neq 0$). In

(26) The number of d–d bands can be rationalized using Tanabe-Sugano diagrams. See, for example: Purcell, K. F.; Kotz, J. C. *Inorganic Chemistry*; W. B. Saunders: Philadelphia, 1977.

(27) Varma, C. A. G. O.; Groenen, E. J. J. *Recl. Trav. Chim. Pays-Bas* **1972**, *91*, 296.

(28) Minkin, V. I.; Osipov, O. A.; Zhdanov, Y. A. *Dipole Moments in Organic Chemistry*; Plenum Press: New York, 1970.

Table IV. The EFISH Measurements at 1.9 μm for Ligands **1** and **2** and for the Corresponding Cobaltous Complexes[a]

	γ_o (10^{-35} esu)		β_z (10^{-30} esu)	
ligands	dioxane	$CHCl_3$	trans	cis
1	80 ± 30	60 ± 25	30 ± 20	10 ± 7
2	200 ± 40	200 ± 40	50 ± 20	40 ± 15
	γ_0 (10^{-35} esu)		β_z (10^{-30} esu)	
complexes	dioxane	$CHCl_3$	dioxane	$CHCl_3$
$Co^{II}(\mathbf{1}^-)_2$	150 ± 30	160 ± 30	25 ± 7	30 ± 8
$Co^{II}(\mathbf{2}^-)_2$	460 ± 90	700 ± 100	70 ± 20	100 ± 25

[a] γ_o is the experimentally observed third harmonic term; β_z is the molecular second harmonic coefficient.

the complexes, these three terms are all different from zero.

The mean microscopic molecular hyperpolarizability may be derived[15] from the macroscopic hyperpolarizability coefficient Γ:

$$\Gamma = Nf\gamma_o$$

N, number of molecules per cm^3

f, product of the local fields

γ_o, microscopic hyperpolarizability

$$\gamma_o = \gamma_e + \frac{\mu_z\beta_z}{5kT}$$

In further calculations the term γ_e will be neglected.[15] In the case where the solution contains a mixture of the cis and trans forms of the ligands, an additive law has been postulated.

Table IV shows the γ_o and β_z values of the ligands and the complexes. The errors on the values of γ_o are 20–40% and 20% for the ligands and the complexes, respectively. The ligand **2** leads to β values approximately two to five times larger than those for conventional nitroaniline derivatives and 10 to 20 times larger than those for urea. The charge transfer state therefore probably involves the whole molecular unit in both the cis and trans isomers. The β values of the complexes determined in dioxane or in chloroform are slightly different. The effect of solvent on the magnitude of β has been recently described.[30] However significant effects are expected only for zwitterionic molecules.

The hyperpolarizability coefficients of the complexes may be estimated theoretically from the corresponding values of the cis ligands by assuming that the contribution of the cobaltous metal ion is negligible (Figure 13).

The hyperpolarizability of the ligands may arise from one- and two-dimensional charge-transfer states. In a ^1D case, only three components must be considered, while the ^2D case leads to eight different components. From the structure determined by X-ray diffraction, the angle between the molecular planes (2α) is approximately 90° for the complex $Co^{II}(\mathbf{2}^-)_2$. By considering a uniaxial charge transfer for the ligands, it follows that

$$\beta_Z = 2\beta_{MS}\cos^3\alpha + 2\beta_{MS}\cos\alpha\sin^2\alpha$$

$$= \sqrt{2}\beta_{MS} \text{ (with } 2\alpha = 90°)$$

where β_Z is the hyperpolarizability coefficient of the complexes arising from a tensorial addition of the hyperpolarizability coefficients of the cis ligands (β_{MS}). β_Z may be readily calculated from the previously measured β_{MS}.

In order to compare the various β values, they have been normalized to eliminate the dispersion effect due to the absorption band present both in the complex and in the ligand. Since an uniaxial charge transfer has been postulated and if this transition involves only two levels then[15]

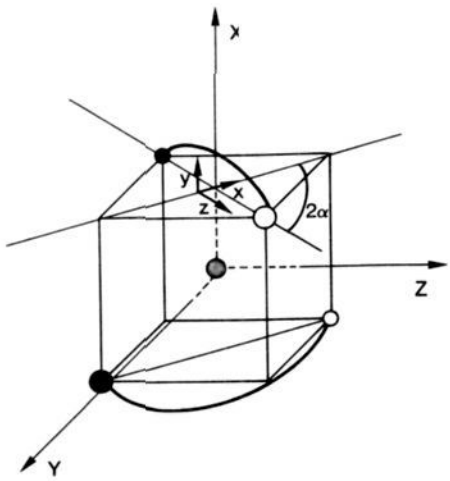

Figure 13. The reference frames used to theoretically estimate the hyperpolarizability coefficients of the complexes from the individual coefficients of the two ligands: x,y,z, molecular axes; XYZ reference frame for the complexes; 2α, angle between the two molecular planes of the ligands.

$$\beta = \frac{\lambda^4}{(\lambda^2 - 4\lambda^2_o)(\lambda^2 - \lambda^2_o)}\beta^\circ$$

with the variables β° and β representing normalized and experimental hyperpolarizability coefficients, respectively; λ, fundamental wavelength; λ = 1.9 μm; λ_o, maximum wavelength of the charge-transfer transition. The results are shown in Table V.

For both complexes $Co^{II}(\mathbf{1}^-)_2$ and $Co^{II}(\mathbf{2}^-)_2$, the experimental β° values seem to be significantly higher (while within experimental errors) than the additive β°_Z values. Overall errors are however indicated (including NMR, μ_g and β determinations), and they are therefore highly overestimated. As an evidence, the values found in two different solvents are very close to each other. Therefore it can be stated that the d-orbitals of the metallic ion play a significant role in the magnitude of β_Z.

Conclusion

A new type of metalloorganic complexes, with highly polarizable ligands, has been synthesized and characterized. The nonlinear optical properties of these complexes demonstrate that the d-orbitals play a significant role in the magnitude of their hyperpolarizability coefficients. The method used (EFISH) for measuring the NLO properties did not permit us to determine the importance of the crossed terms (such as β_{XYZ}) on this effect.

It is however not possible at this stage to determine which parameters are altered by the presence of a metallic ion: (i) a better delocalization within the ligands induced by the d-orbitals of the metal ion, (ii) the appearance of nonnegligible crossed terms due to a ^3D charge-transfer state, and (iii) a contribution from an interligand charge-transfer process within the complexes. Studies are under progress to elucidate this point.

Experimental Section

The following equipment was used for characterizing the compounds synthesized: NMR spectra (Brucker AC ^1H 200 MHz, ^{13}C 50 MHz); IR (KBr discs), (Perkin Elmer 1600 FTIR); UV–vis (Uvikon 860); and near-IR (Beckman UV 5240). The microanalyses were performed at ICS-Strasbourg. The error bars indicated in Tables II and III take into

Table V. The Normalized Hyperpolarizability Coefficients of the Cis Ligands and of the Corresponding Colbaltous Complexes, Determined in Chloroform

ligands	λ_o (nm)	β°_{MS} (10^{-30} esu)	complexes	λ_o (nm)	β° (10^{-30} esu)	$\beta^\circ_Z = \sqrt{2}\beta^\circ_{MS}$ (10^{-30} esu)
1	414	8 ± 6	$Co^{II}(\mathbf{1}^-)_2$	478	21 ± 6	11 ± 8
2	459	30 ± 10	$Co^{II}(\mathbf{2}^-)_2$	518	65 ± 20	40 ± 15

Table VI

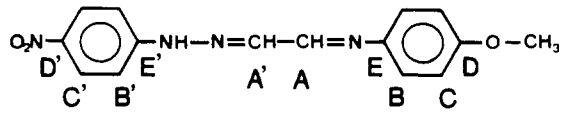

	C′	($J_{B'C'}$)[a]	B′	NH	A′	($J_{A'A}$)	A	B	(J_{BC})	C	OMe
DMSO-d_6 (trans)	8.18	(9.2)	7.21	11.7	7.83	(8.1)	8.37	7.33	(8.8)	6.96	3.78
$CDCl_3$ (cis)				14.7	7.05	(2.1)	8.11				

[a] Value in Hz. Chemical shift in ppm downfield from TMS.

Table VII

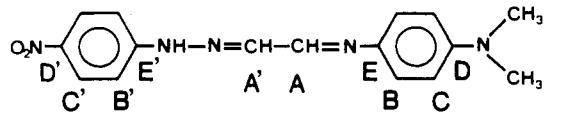

	C′	($J_{B'C'}$)	B′	NH	A′	($J_{A'A}$)	A	B	(J_{BC})	C	$-NMe_2$
DMSO-d_6 (trans)	8.18	(9.2)	7.19	11.65	7.83	(8.1)	8.38	7.29	(9.0)	6.73	2.93
$CDCl_3$ (cis)				14.8	7.01	(1.9)	8.12				

account (i) the systematic error and correlation accuracy of the dielectric measurements used for calculating μ_g and (ii) the error concerning the ratio of the cis-to-trans isomer as measured by NMR. In Tables IV and V, the errors introduced when measuring the β values have also been added.

Synthesis of the Ligands. *p*-Nitrophenylhydrazine (**3**) is commercially available (Aldrich) and was used without further purification. The glyoxal derivative (**5**) of *p*-nitrophenylhydrazine was prepared following a method modified from an already published procedure.[17,31-33]

Compound 5. *p*-Nitrophenylhydrazine (**3**) (37.5 g, 0.245 mol) was dissolved at room temperature in acetic acid (1000 cm^3). A solution of glyoxal in water (21.28 g, 0.367 mol in 1280 cm^3 water) was prepared, and the acetic solution was added dropwise at room temperature. A reddish precipitate immediately formed. On complete addition (40 mn), the mixture was stirred for 2 h at room temperature. The precipitate was then filtered off, washed with water (4 × 500 cm^3), and dried under vacuum (crude yield: 92%). On cooling (4 °C) the filtrate, further orange product (0.9 g) was precipitated and collected.

5: mw 193.16; ^{1}H NMR (200 MHz, DMSO-d^6) 7.35 (d, arom, 2 H, J = 9.1 Hz), 7.47 (d, —CH=N—, 1 H, J = 7.8 Hz), 8.24 (d, arom, 2 H, J = 9.1 Hz), 9.55 (d, –CHO, 1 H, J = 7.8 Hz), 12.0 (br s, –NH–, 1 H); mw, 193.16. Anal. Calcd for $C_8H_7N_3O_3$: C, 49.7; H, 3.6; N, 21.7. Found: C, 48.7; H, 3.6; N, 21.2.

A second experimental procedure was also used to synthesize **5**.

p-Nitrophenylhydrazine (**3**) (22.17g, 0.145 mol) was dissolved in DMSO (50 cm^3) at room temperature, and then added dropwise to an aqueous solution of glyoxal (16.76 g, 0.289 mol, in 400 cm^3 water) at room temperature. After completion of the addition, the mixture was stirred for 30 mn. The precipitate which formed was filtered off at room temperature, washed with water (5 × 250 cm^3), and dried under vacuum at 50 °C (crude yield, 95%).

1-((*p*-Nitrophenyl)hydrazono-2-((*p*-methoxyphenyl)imino)ethane (1). The experimental procedure employed was modified from that described in ref 17. A description of structurally related ligands can be found in the literature.[24,25,34-36]

The monosubstituted glyoxal derivative **5** (7.24 g, 30 mmol) was dissolved in DMSO (80 cm^3) at 70 °C. To this solution, *p*-anisidine (Aldrich) (3.69 g, 33 mmol) in DMSO (10 cm^3) was added dropwise at room temperature. The reaction mixture was stirred at room temperature for 3 h and, on completion of the reaction, was heated to 70 °C. Water was then added (10 cm^3), and, on cooling to room temperature, the orange product precipitated. The product was then filtered off, washed with water, and dried under vacuum (crude product: quantitative yield). Recrystallization of the product from absolute ethanol gave 3.58 g of pure compound (yield, 40%), mp 252 °C (lit.[17] 209–210 °C).

1: mw 298.30; ^{1}H NMR (200 MHz) (see Table VI); ^{13}C NMR (50 MHz) DMSO-d_6 (trans) D′, 141.9; C′, 125.9; B′, 112.0; E′, 149.3; A′ 143.1; A, 158.3; E, 155.3; B, 122.5; C, 114.3; D, 139.5; OMe, 55.1; IR (KBr, in cm^{-1}) 1599.0, 1554.2, 1503.8, 1332.3, 1289.7, 1280.0, 1109.7, 841.0, 749.8, 530.8; UV (λ_{max} in nm, ϵ_{max} in mol^{-1} dm^3 cm^{-1}) EtOH, neutral form 305 s, 340 s, 404 (41 500); EtOH, basic form 342 s, 385 (10 800), 552 (45 200); dioxane 300 s, 340 s, 401 (49 500); $CHCl_3$ 315 s, 342 s, 414 (38 000). Anal. Calcd for $C_{15}H_{14}N_4O_3$: C, 60.40; H, 4.73; N, 18.78. Found: C, 60.19; H, 4.64; N, 18.52.

1-((*p*-Nitrophenyl)hydrazono)-2-((*p*-dimethylamino)phenyl)imino)-ethane (2). The same procedure as used for **1** was followed. The crude product which was obtained in quantitative yield was recrystallized in ethanol (yield 35%; mp 261 °C).

2: mw 311.34; ^{1}H NMR (200 MHz) (see Table VII); ^{13}C NMR (50 MHz) DMSO-d_6 (trans) D′, 139.4; C′, 126.1; B′, 112.0; E′, 149.6; A′, 142.9; A, 151.9; E, 149.8; B, 122.7; C, 112.4; D, 138.8; –NMe_2, 40.4; IR (KBr, in cm^{-1}) 1609.3, 1596.5, 1560.5, 1502.0, 1324.4, 1300.1, 1281.9, 1109.2, 838.6, 747.9, 527.6; UV (λ_{max} in nm, ϵ_{max} in mol^{-1} dm^3 cm^{-1}) EtOH, neutral form 338 s, 375 s, 436 (47 800); EtOH, basic form 370 s, 396 (12 800), 565 (55 600); dioxane 340 s, 375 s, 434 (44 500); $CHCl_3$ 345 s, 392 s, 459 (35 500). Anal. Calcd for $C_{16}H_{17}N_5O_2$: C, 61.72; H, 5.50; N, 22.49. Found: C, 61.8; H, 5.5; N, 22.4.

Synthesis of the Complexes. $Co^{II}(1^-)_2$. **1** (1 g, 3.35 mmol) was heated with stirring at 70 °C in ethanol (100 cm^3), and a solution of potassium ethoxide (1 M in ethanol, 3.35 mL) was added. Immediately, the violet color characteristic of 1^- appeared, and the solution became homogeneous. $Co(AcO)_2$ (0.33 g, 1.84 mmol), previously dehydrated from $Co(AcO)_2 \cdot 4H_2O$ under vacuum at 150 °C, was then added to the reaction mixture, followed immediately by the disappearance of violet coloration and the formation of a brown precipitate. The precipitate was then filtered off and washed with ethanol. The product $Co^{II}(1^-)_2$ was solubilized in CH_2Cl_2 (20 cm^3) and filtered to remove the salt present in excess. The crude product was recrystallized from a mixture AcOEt/EtOH (1:1 v/v) giving 0.82 g (75%) as green needles with a metallic lustre: TLC, SiO_2, eluent, $CHCl_3$/EtOH (98/2); R_f 0.8.

$Co^{II}(1^-)_2$: mw 653.52; IR (KBr, in cm^{-1}), 1605.1, 1586.2, 1505.4, 1457.8, 1322.1, 1231.8, 1150.8, 1106.4, 1016.1, 994.7, 848.2, 753.8, 693.1; UV NIR (λ_{max} in nm, ϵ_{max} in mol^{-1} dm^3 cm^{-1}) CH_2Cl_2 365 s, 478 (54 200), 625 s, 690 (2450), 1020 (77); dioxane 360 s, 471 (52 100), 625 s, 687 (2410), 1020 (80); $CHCl_3$ 300 s, 365 s, 478 (55 900), 613 s, 691 (2650), 1010 (81). Anal. Calcd for $C_{30}H_{26}N_8O_6Co$: C, 55.14; H, 4.01; N, 17.15; Co, 9.02. Found: C, 55.31; H, 3.96; N, 17.16; Co, 8.89.

$Ni^{II}(1^-)_2$. The same procedure as above was followed: salt, $NiBr_2 \cdot 3H_2O$ (dried at 200 °C under vacuum). The reaction mixture was stirred under reflux for 3 h. At room temperature, the precipitate was collected and extracted with acetone. The crude product was recrystallized from a mixture acetone/ethanol giving green needles: yield 20%; TLC same as above; R_f 0.8.

$Ni^{II}(1^-)_2$: mw 653.30; IR (KBr, in cm^{-1}) 1605.7, 1585.9, 1505.0, 1460.8, 1330.1, 1318.3, 1226.9, 1152.3, 1102.1, 1025.6, 845.9, 751.5, 693.5; UV NIR (λ_{max} in nm, ϵ_{max} in mol^{-1} dm^3 cm^{-1}) CH_2Cl_2 362 s, 461 (46 300), 650 s, 1110 (47), 1250 s. Anal. Calcd for $C_{30}H_{26}N_8O_6Ni$: C,

(29) Paley, M. S.; Harris, J. M.; Looser, H.; Baumert, J. C.; Bjorklund, G. C.; Jundt, D.; Twieg, R. J. *J. Org. Chem.* **1989**, *54*, 3774.
(30) Marder, S. R.; Beratan, D. N.; Cheng, L.-T. *Science* **1991**, *252*, 103.
(31) Reich, H.; Helfe, L., Jr. *J. Org. Chem.* **1956**, *21*, 708.
(32) Stepanov, B. I.; Avramenko, G. V.; Shandurenko, G. V. *USSR Patent* 727,635, 1978; *Chem. Abstr.* 93: 185139j.
(33) Newton, T. W.; McArthur, A. *Brit. UK Patent GB* 2,193,493 1986; *Chem. Abstr.* 108: 204628u.
(34) McNab, H. *J. Chem. Soc., Perkin Trans. I* **1978**, *9*, 1023; **1982**, *8*, 1941.
(35) McNab, H.; Smith, G. S. *J. Chem. Soc., Chem. Commun.* **1982**, *17*, 996.
(36) McNab, H. *J. Chem. Soc., Perkin Trans I* **1984**, *3*, 377.

55.16; H, 4.01; N, 17.15; Ni, 8.99. Found: C, 55.33; H, 3.97; N, 17.20; Ni, 9.87.

$Cu^{II}(1^-)_2$. The same procedure was followed as above: salt, $Cu(CF_3SO_3)_2$ (dried at 150 °C under vacuum). The black precipitate formed was washed with ethanol: yield 75%; TLC same as above; R_f 0.7.

$Cu^{II}(1^-)_2$: mw 658.13; IR (KBr, in cm^{-1}) 1604.9, 1585.4, 1503.9, 1457.2, 1329.8, 1318.1, 1237.8, 1159.7, 1100.6, 1020.0, 846.2, 751.2, 692.4; UV NIR (λ_{max} in nm, ϵ_{max} in mol^{-1} dm^3 cm^{-1}) CH_2Cl_2 360 s, 422 s, 465 (39 700), 490 s, 679 (2490), 1330 (210). Anal. Calcd for $C_{30}H_{26}N_8O_6Cu$: C, 54.75; H, 3.98; N, 17.02; Cu, 9.65. Found: C, 54.58; H, 3.92; N, 16.90; Cu, 9.88.

$Co^{II}(2^-)_2$. The same procedure was followed as for $Co^{II}(1^-)_2$: recrystallization, AcOEt (yield 60%). The X-ray structure was determined on a single crystal grown in benzene.

$Co^{II}(2^-)_2$: mw 679.61; IR (KBr, in cm^{-1}) 1607.3, 1584.9, 1498.4, 1458.5, 1319.2, 1237.8, 1143.9, 1101.9, 1021.4, 998.1, 849.5, 752.9, 693.7; UV NIR (λ_{max} in nm, ϵ_{max} in mol^{-1} dm^3 cm^{-1}) CH_2Cl_2 340 s, 397 s, 518 (53 800), 670 s, 1020 (74); dioxane 340 s, 385 s, 506 (52 000), 655 s, 1020 (75); $CHCl_3$ 335 s, 390 s, 518 (53 300), 670 s, 1010 (76). Anal. Calcd for $C_{32}H_{32}N_{10}O_4Co$: C, 56.56; H, 4.75; N, 20.61; Co, 8.67. Found: C, 56.51; H, 4.75; N, 20.65; Co, 8.57.

Determination of the Ground-State Dipole Moments. Ground-state dipole moments were measured at Thomson using an in-house apparatus following ref 37. The solutions (benzene, chloroform, dioxane) were in the range 10^{-2}–10^{-3} M. The refractive index of the solutions was measured using an Abbe's refractometer (OPL).

The dipole moments are determined by the measurement of the capacitance C_p of a condenser, in which the dielectric is a solution of the molecular compound to be studied. The dielectric constant of the solution ϵ_{12} (1; solvent; 2, solute) is given by

$$C_p = A\epsilon_{12} + B$$

A,B: cell constants

C_p in pF

Various relationships can be found for expressing ϵ_{12} as a function of the molecular dipole moment of the solute.[28,38] In the general case where the solute is dissolved in a polar solvent, the relationship is[28]

$$C_2(P_2 - P_1) + P1/\bar{V} = [(\epsilon_{12} - 1)(\epsilon_{12} + 2)/8\epsilon_{12} - (n_{12}^2 - 1)(n_{12}^2 + 2)/8n_{12}^2]$$

with P_1, P_2, molar polarizations due to the solvent or the solute, respectively; C_2, concentration of the solute (in mol per unit volume of solution) ($C_2 = x_2/\bar{V}$); ϵ_{12}, n_{12}, dielectric constant and refractive index of the solution, respectively; $\bar{V}$, molar volume of the solution;

$$\bar{V} = \frac{M_1x_1 + M_2x_2}{d_{12}}$$

d_{12}, density of the solution; M_1,M_2, molecular weights of the solvent and solute, respectively; x_1,x_2, mole fractions of the solvent (N_1 mol) and solute (N_2 mol), respectively.

$$x_1 = \frac{N_1}{N_1 + N_2}$$

$$x_2 = \frac{N_2}{N_1 + N_2}$$

In the calculations, $\bar{V}$ will be considered to be constant, i.e., for dilute solutions, the molar volume is not significantly changed when the concentration of the solute is varied. P_1 may be easily calculated knowing the dielectric constant ϵ_1 and the refractive index n_1 of the pure solvent. $P_2 - P_1$ is the slope of the curve $f(\epsilon_{12}, n_{12})$ vs C_2, when C_2 is varied. The molecular dipole moment of the solute may be then calculated, since

$$P_2 = \frac{4}{9}\pi\mathcal{N}\frac{\mu_2^2}{kT}$$

with the following constants being $\mathcal{N}$, Avogadro's number (6.02×10^{23}); μ_2, dipole moment in esu-cm (1D = 10^{-18} esu-cm); k, Boltzmann constant ($k = 1.38 \times 10^{-16}$ erg·K^{-1}); and $\epsilon_0 = 1/4\pi$; dielectric constant of vacuum.

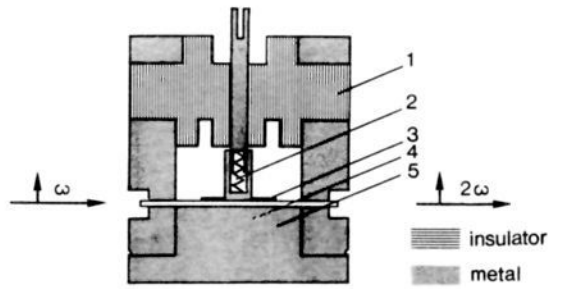

Figure 14. Schematic representation of the cell used for determining SHG: 1, cell cover; 2, spring; 3, upper electrode; 4, quartz window (2 mm); and 5, lower electrode.

NLO Measurements. NLO measurements were carried out at Strasbourg (IPCMS) with an in-house apparatus.

The laser source used had the same specifications as those described in ref 15. The 1.9 μm radiation was obtained with a Raman cell containing hydrogen.

The fundamental beam was polarized vertically and focussed in the cell with a lens (50–60 cm focal distance.) A schematic representation of the cell made and used in Strasbourg is shown in Figure 14.

In this configuration the static field is uniform in the active part of the cell. A pulsed electric field with the same polarization as the incident laser beam was used (10 μs, 5 kV) to orientate the solute molecules within the solvent. The field and the laser beam were synchronized with a Q-switch.

X-ray Determination. The X-ray diffraction was performed with an Enraf-Nonius CAD-4 spectrometer at the Université P. et M. Curie (Jussieu) $C_{32}H_{32}N_{10}O_4Co$; mw 679.607; number of unique data used 3230; R = 3.7%; triclinic ($P\bar{1}$) a = 10.819 Å, b = 11.645 Å, c = 13.991 Å, α = 86.40°, β = 84.97°, γ = 70.56°, Z = 2, ρ(calcd) = 1.364 g/cm^3.

Acknowledgment. A part of this work was conducted at the Research Center of the "Société Française Hoechst" by one of us. We acknowledged the staff of this company and especially Dr Blanc and Dr Mattioda for their scientific contribution and for financial support. Thomson and CNET are thanked for the determination of the ground-state dipole moments and preliminary NLO studies, respectively. F. Robert is thanked for the X-ray determination and helpful discussions.

Registry No. 1, 75119-96-9; $Co^{II}(1^-)_2$, 138093-31-9; $Cu^{II}(1^-)_2$, 138093-33-1; $Ni^{II}(1^-)_2$, 138093-32-0; **2**, 138093-11-5; $Co^{II}(2^-)_2$, 138093-34-2; **3**, 100-16-3; **4**, 107-22-2; **5**, 3078-12-4; MeO-*p*-$C_6H_4NH_2$, 104-94-9; Me_2N-*p*-$C_6H_4NH_2$, 99-98-9.

Supplementary Material Available: ORTEP figure and tables of crystal data, atomic and thermal parameters, anisotropic thermal parameters, and bond lengths and angles (7 pages). Ordering information is given on any current masthead page.

(37) Janini, G. M.; Katrib, A. H. *J. Chem. Ed.* **1983**, *60*, 1087.
(38) Guggenheim, E. A. *Trans. Faraday Soc.* **1949**, *45*, 714.